Evaluation of an entraining droplet activation parameterization using in situ cloud data

R. Morales,[1] A. Nenes,[1,2] H. Jonsson,[3] R. C. Flagan,[4] and J. H. Seinfeld[4]

Received 13 November 2010; revised 28 April 2011; accepted 17 May 2011; published 10 August 2011.

[1] This study investigates the ability of a droplet activation parameterization (which considers the effects of entrainment and mixing) to reproduce observed cloud droplet number concentration (CDNC) in ambient clouds. Predictions of the parameterization are compared against cloud averages of CDNC from ambient cumulus and stratocumulus clouds sampled during CRYSTAL-FACE (Key West, Florida, July 2002) and CSTRIPE (Monterey, California, July 2003), respectively. The entrainment parameters required by the parameterization are derived from the observed liquid water content profiles. For the cumulus clouds considered in the study, CDNC is overpredicted by 45% with the adiabatic parameterization. When entrainment is accounted for, the predicted CDNC agrees within 3.5%. Cloud-averaged CDNC for stratocumulus clouds is well captured when entrainment is not considered. In all cases considered, the entraining parameterization compared favorably against a statistical correlation developed from observations to treat entrainment effects on droplet number. These results suggest that including entrainment effects in the calculation of CDNC, as presented here, could address important overprediction biases associated with using adiabatic CDNC to represent cloud-scale average values.

Citation: Morales, R., A. Nenes, H. Jonsson, R. C. Flagan, and J. H. Seinfeld (2011), Evaluation of an entraining droplet activation parameterization using in situ cloud data, *J. Geophys. Res.*, *116*, D15205, doi:10.1029/2010JD015324.

1. Introduction

[2] Activation of atmospheric particles (termed cloud condensation nuclei, or CCN) by condensation of water vapor to form cloud droplets is the direct microphysical link between aerosols and clouds. Modifications in either the concentration or composition of atmospheric CCN can affect cloud microphysical properties. An increase in aerosol concentration, for example, generally leads to an increase in cloud droplet number concentration (CDNC), with subsequent impacts on cloud thickness, cloud albedo and precipitation [*Intergovernmental Panel on Climate Change*, 2007]. Aerosol-cloud interactions are amongst the most challenging of atmospheric processes to predict, because of the dynamical, microphysical and macrophysical feedbacks that occur across a wide range of temporal and spatial scales (which often operate at the subgrid scale in global climate models, GCMs) [*Stevens and Feingold*, 2009]. Nevertheless, a realistic representation of aerosol-cloud interactions is necessary for improved assessments of climate change.

[3] Cloud microphysical properties in most GCM studies are determined based on the resolved liquid water content (q_l, kg kg^{-1}) and a parameterization of CDNC (N_d, cm^{-3}). These two variables are used to express the cloud microphysical characteristics relevant for cloud processes and radiative forcing calculations, such as effective radius of the droplet population, dispersion of the droplet size distribution [e.g., *Liu et al.*, 2008], and autoconversion rate [e.g., *Khairoutdinov and Kogan*, 2000]. Cloud schemes that include two-moment microphysics are based on solving prognostic equations for q_l and N_d, which relate both variables to an assumed droplet size distribution, the first and third moments of which are constrained by N_d and q_l, respectively [e.g., *Morrison and Gettelman*, 2008].

[4] The need for accurate but computationally efficient representations of the droplet activation process in GCMs has lead to a large body of work [e.g., *Twomey*, 1959; *Abdul-Razzak et al.*, 1998; *Nenes and Seinfeld*, 2003; *Fountoukis and Nenes*, 2005; *Ming et al.*, 2006]. These activation parameterizations are based on approximate solutions of the coupled mass and energy balances for an ascending Lagrangian cloud parcel, during which a population of particles activates to cloud droplets. This framework allows the calculation of water vapor supersaturation; a maximum value, s_m, is reached when the availability of water vapor from expansion cooling is equal to the loss from condensation onto the nucleated droplets. Knowledge of s_m is then used to determine the nucleated droplet number (that is, the number concentration of particles with critical supersaturation less than s_m). A thorough review and evaluation of activation parameterizations is provided by S. J. Ghan et al. (Droplet

[1]School of Earth and Atmospheric Sciences, Georgia Institute of Technology, Atlanta, Georgia, USA.
[2]School of Chemical and Biomolecular Engineering, Georgia Institute of Technology, Atlanta, Georgia, USA.
[3]Center for Interdisciplinary Remotely Piloted Aircraft Studies, Naval Postgraduate School, Monterey, California, USA.
[4]Department of Chemical Engineering and Department of Environmental Science and Engineering, California Institute of Technology, Pasadena, California, USA.

0148-0227/11/2010JD015324

nucleation: Physically-based parameterization and comparative evaluation, submitted to *Journal of Advances in Modeling Earth Systems*, 2010).

[5] Entrainment has been long recognized as an important process shaping the droplet number concentration and size distribution of cloud droplets [e.g., *Warner*, 1973; *Lehmann et al.*, 2009]. Mixing of cloud-free air in cloud is thought to occur in entrained "pockets" with a characteristic length scale of the order of the cloud itself, driven by the convective circulation in the cloud. The entrained air is then turbulently mixed with the cloudy air in a cascade of eddies down to the Kolmogorov scale, where molecular diffusion dominates transport [*Krueger et al.*, 1997]. The ratio of evaporation and turbulent mixing timescales has been found to determine the impact of the mixing process on the droplet size distribution and the CDNC [*Latham and Reed*, 1977; *Baker et al.*, 1980]. When the timescale of evaporation is much longer than that of turbulent mixing, all droplets are effectively exposed to the same supersaturation, partially evaporate, and then decrease in size at more or less constant CDNC ("homogeneous mixing"). Conversely, if the mixing process is slower than the evaporation process and well-defined interfaces between cloudy and clear air "pockets" are maintained sufficiently long, droplets surrounded by entrained air completely evaporate, while those surrounded by saturated cloudy air remain largely unaffected ("Inhomogeneous mixing"). At the inhomogeneous mixing limit, CDNC is depleted, while the shape of the droplet size distribution is essentially unchanged. Observations suggest that both entrainment mechanisms occur [e.g., *Burnet and Brenguier*, 2006]. For a particular cloud, a length scale exists below which mixing is predominantly homogeneous, and above which mixing is inhomogeneous [*Lehmann et al.*, 2009]. Both mixing limits have been explored in modeling studies [e.g., *Krueger et al.*, 1997; *Lasher-Trapp et al.*, 2005]. Modeling studies also suggest that entrainment-mixing effects may substantially affect the simulated albedo of clouds [*Chosson et al.*, 2006].

[6] Cloud schemes in GCMs are often one-dimensional representations of clouds (i.e., with homogeneous characteristic across a horizontal section of the cloud), often based on the entraining plume concept that adopt the model of lateral entrainment and mixing [e.g., *Tiedtke*, 1989; *de Rooy and Siebesma*, 2010]. They do not however account for entrainment impacts on droplet number, which is generally considered beyond the reach of GCM cloud schemes. Empirical approaches based on observations, which inherently include entrainment effects, have been proposed to circumvent this issue. *Leaitch et al.* [1996] derived such a correlation from marine stratus cloud observations, that link adiabatic to cloud average CDNC. The relationship has seen application in the ECHAM model to represent entrainment effects on convective cloud microphysics [*Lohmann*, 2008]. Apart from such empirical approaches, other GCM schemes use adiabatic CDNC to represent the cloud-scale average CDNC, hence are subject to overprediction biases. *Barahona and Nenes* [2007, hereinafter BN07] explored the implication of continuous, homogeneous mixing during the activation process, and developed a mechanistic parameterization that includes the effects of entrainment on the number of nucleated cloud droplets. Assuming that droplet concentrations predicted with BN07 represents cloud-scale average CDNC, *Barahona et al.* [2011] applied the parameterization within a global model simulation (using a variety of approaches to represent entrainment) and was found to improve the representation of spatial patterns of CDNC and cloud droplet effective radius. BN07 however has not been tested against in situ measurements, particularly in combination with approaches to determine entrainment rates that are consistent with observed liquid water content profiles.

[7] The focus of this work is to investigate the ability of the BN07 activation parameterization to reproduce cloud-scale average CDNC observed in ambient clouds. We focus on two major types of warm clouds, cumulus and stratocumulus. Unlike previous studies that evaluate parameterizations with observations at cloud base or for near-adiabatic parcels, closure is assessed for cloud average values of CDNC (which is what is required in GCM simulations). To avoid biases in the observed CDNC resulting from droplet collision and coalescence, the study is carried out for clouds in the absence of substantial amounts of drizzle.

2. The Conceptual Framework

[8] Entrainment and mixing is likely to deplete the liquid water content and the CDNC through the entire cloud column; this implies that at the cloud scale, neither variable will be adequately represented by adiabatically calculated values (although the latter can closely approximate values near cloud base [*Meskhidze et al.*, 2005]). CDNC predicted with an entraining parameterization could however more realistically represent the cloud scale average CDNC, especially if the entrainment rate applied is consistent with the vertical profile of cloud liquid water. This conceptual framework is presented in Figure 1; assuming adiabatic CDNC throughout the cloud column tends to overpredict the quantity on average when compared against observations (symbols).Using BN07 to predict the average cloud column CDNC can lead to better agreement with observations (given the appropriate entrainment rate).

[9] BN07 adopts the continuously entraining, homogeneous mixing model [*Pruppacher and Klett*, 1997] to compute droplet number; it involves a Lagrangian parcel of cloudy air which is allowed to exchange mass with the environment at a per unit length entrainment rate e (m^{-1}). The environmental air is characterized by its temperature and water vapor mixing ratio, T' and q'_v respectively. As the parcel ascends, supersaturation is initially generated and cloud droplets nucleate until mixing and water condensation dominate over water availability from expansion cooling. The resulting activated CDNC is subsequently applied uniformly in the vertical (Figure 1).

[10] The entrainment model adopted in BN07 was developed for cumulus convection; we therefore expect the predicted CDNC with this formulation to better reproduce observations of small cumulus clouds than the stratocumulus cloud cases, where the entrainment process has a different structure and cloud microphysical impacts. For completeness however we test the entraining parameterization for both cloud types. In the following sections we describe the activation parameterization and its application to represent the average CDNC in ambient clouds. Different strategies to diagnose the effective entrainment rate from observed liquid water content profiles are developed. Quantitative implica-

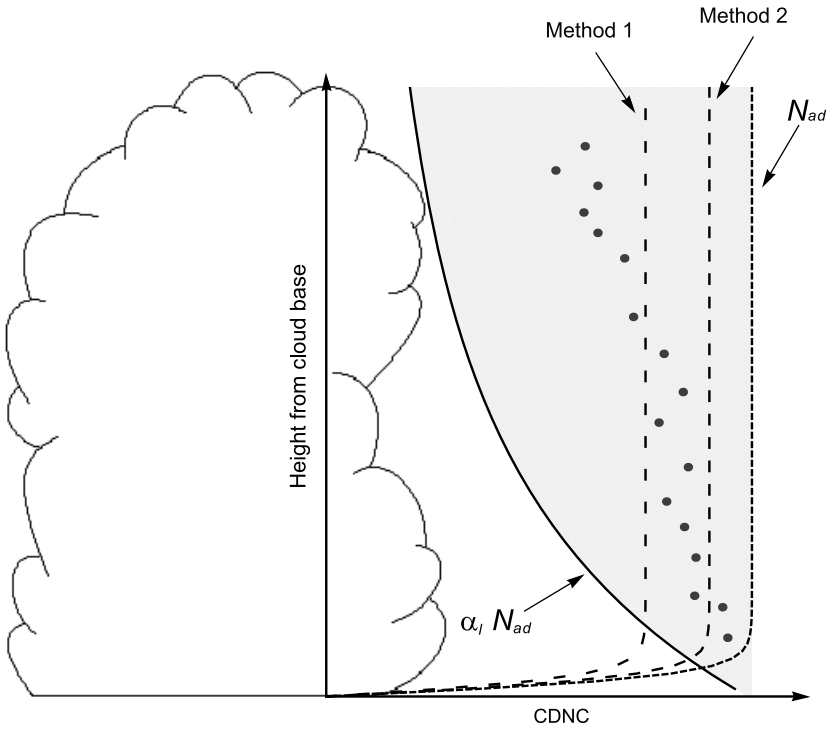

Figure 1. Schematic of the expected impact of predicted CDNC with the different approaches discussed in the text. The points represent actual observed CDNC, while the shaded area represents the region bounded by the adiabatic (N_{ad}) and inhomogeneous mixing limits ($\alpha_l N_{ad}$). Dashed lines represent CDNC predicted with BN07 when $(1 - e/e_c) \sim \alpha_{l,avg}$ and $(1 - e/e_c)$ derived from least square fits to observed α_l profiles.

tions of entrainment on the predicted CDNC and effective radius are provided and discussed within the context of published literature.

2.1. The Entraining Activation Parameterization

[11] BN07 is an extension of the work of *Nenes and Seinfeld* [2003] and *Fountoukis and Nenes* [2005, hereinafter FN05]; it can treat the effects of externally mixed aerosol, CCN containing partially soluble compounds and surfactants that affect surface tension and facilitate activation, and delays in activation kinetics from the presence of film-forming compounds and slowly dissolving compounds. The parameterization has also been extended to include droplet formation from adsorption activation of insoluble aerosol (e.g., dust) [*Kumar et al.*, 2009] and a detailed consideration of water vapor depletion from large and giant CCN [*Barahona et al.*, 2010]. BN07 accurately reproduces detailed parcel model simulations. Its adiabatic counterpart, FN05, has been shown to reproduce CDNC for nearly adiabatic conditions in cloud base transects sampled in ambient cumulus and stratocumulus clouds [*Meskhidze et al.*, 2005; *Fountoukis et al.*, 2007].

[12] BN07 is based on the rate of change of the supersaturation, s, in the entraining cloud parcel [*Pruppacher and Klett*, 1997; *Barahona and Nenes*, 2007],

$$\frac{ds}{dt} = \alpha w\left[1 - \frac{e}{\alpha}\left(\frac{q_v - q_v'}{q_v} - \frac{M_w \Delta H \Delta T}{RT^2}\right)\right] - \gamma\left(\frac{dq_l}{dt}\right)_c \quad (1)$$

where $(dq_l/dt)_c$ is the condensation rate of water into the droplets, $\alpha = \frac{gM_w\Delta H}{c_p RT^2} - \frac{gM_a}{RT}$, $\gamma = \frac{pM_a}{p^o(T)M_w} + \frac{M_w\Delta H}{c_p RT^2}$, w is the updraft velocity of the parcel, M_a and M_w are the molecular weights of air and water, respectively, ΔH is the heat of vaporization of water, c_p is the specific heat capacity of air, g is the gravitational acceleration, p is the pressure, $p^o(T)$ is the saturation vapor pressure, and R is the universal gas constant. The terms in brackets represent the effects of the entrainment in the parcel supersaturation, where q_v' is the water vapor mixing ratio of the entrained air, and $\Delta T = T - T'$ is the difference between the parcel and environmental temperatures.

[13] Fundamental to BN07 is the concept of the *critical entrainment rate*, e_c, defined as the entrainment rate above which cloud formation is prevented by excessive dilution of the ascending parcel by environmental air [*Barahona and Nenes*, 2007]. Under aerosol mass concentrations $\leq$100 μg m^{-3}, where the water condensed on the aerosol before saturation can be neglected, e_c was shown to be $e_c = \alpha q_{vs}(q_{vs} - q_v' - \frac{\Delta H M_w q_{vs} \Delta T}{RT^2})^{-1}$, where q_{vs} is the saturation mixing ratio (i.e., e_c is equal to the reciprocal of the factor multiplying e in equation (1) evaluated at saturation). With these definitions, and near cloud base, equation (1) can be written as

$$\frac{ds}{dt} = (1 - e/e_c)\alpha w - \gamma\left(\frac{dq_l}{dt}\right)_c \quad (2)$$

[14] This expression describes how the mixing during the droplet activation process can decrease the maximum supersaturation (and therefore the CDNC) compared to activation under adiabatic conditions. Most physically based droplet activation parameterizations calculate the adiabatic CDNC by determining the maximum supersaturation, s_m, that develops in the cloudy parcel (thus solving $(ds/dt) = 0$ in equation (2) for $e = 0$). Based on equation (2) BN07 showed that any adiabatic activation parameterization (based on equation (2) for $e = 0$) can account for the effects of entrainment on CDNC if the updraft velocity w is replaced with $(1 - e/e_c)w$ in an adiabatic calculation. This operational modification does not imply that the physical updraft w is decreased, but accounts for the decrease in the water vapor availability as expressed in the first term of the right hand side of equation (1) or equation (2).

[15] Different methods to infer the entrainment parameter $(1 - e/e_c)$ from cloud observations are discussed in section 2.2, and a quantitative description of the expected effects of this modification in the predicted CDNC, N_d, is provided in section 2.3.

2.2. Determination of the Entrainment Parameters

[16] Application of BN07 requires specification of $(1 - e/e_c)$; this quantity can be estimated from liquid water content (LWC) profile observations if a relation between $q_l(z)$ and the entrainment parameter $(1 - e/e_c)$ can be established. Assuming that all the water vapor in excess of saturation condenses in the ascending parcel (appropriate for warm clouds where supersaturation rarely exceeds 1%), s and ds/dt in cloud are identically zero. The vertical distribution of (subadiabatic) liquid water can then be determined from equation (2). This is done by setting $ds/dt = 0$, solving the resulting equation for $(dq_l/dt)_c$, and noticing that the total change in the liquid water content (dq_l/dt) includes the sum of the condensation rate $(dq_l/dt)_c$ and the dilution from entrainment of noncloudy air, $(dq_l/dt)_{dil} = -ewq_l$. Finally, considering that $w(dq_l/dz) = (dq_l/dt)$, the resulting expression is

$$\frac{dq_l}{dz} = \Gamma_{l,ad}(1 - e/e_c) - eq_l \tag{3}$$

where z is the vertical coordinate and $\Gamma_{l,ad} = \alpha/\gamma$ is the adiabatic liquid water content lapse rate (given by equation (2) for $e = 0$). If $\Gamma_{l,ad}$ and e/e_c are assumed constant with height, equation (2) can be analytically integrated from cloud base height z_{cb} (the height where saturation is reached, such that $q_l(z) > 0$ for $z \geq z_{cb}$) to a height z. The integrated solution can be expressed in terms of the *dilution ratio*, α_l, the ratio of $q_l(z)$ to the adiabatic liquid water mixing ratio, $q_{l,ad} = \Gamma_{l,ad}(z - z_{cb})$,

$$\alpha_l(z) = \frac{q_l(z)}{q_{l,ad}(z)} = (1 - e/e_c)\frac{1 - \exp[-e(z - z_{cb})]}{e(z - z_{cb})} \tag{4}$$

[17] Despite its simplifications, equation (4) qualitatively reproduces some characteristics of observed α_l profiles. For all in-cloud heights $z \geq z_{cb}$, $\alpha(z) \leq 1$, and in particular, $\alpha(z) \leq (1 - e/e_c)$. Equation (4) also implies that for small in-cloud heights (i.e., $e(z - z_{cb}) \ll 1$), $\alpha_l(z) \approx (1 - e/e_c)$, while higher up in the cloud $\alpha_l \sim (z - z_{cb})^{-1}$. This is consistent with observational studies that show a decrease in α_l with height [e.g., *Warner*, 1970; *Peng et al.*, 2002; *Lu et al.*, 2008].

[18] Equation (4) also suggests that measurements of α_l could provide the basis for inferring $(1 - e/e_c)$. In principle, observations of α_l near cloud base (i.e., $e(z - z_{cb}) \ll 1$) are approximately equal to $(1 - e/e_c)$. However, such measurements are sensitive to the choice of z_{cb} (which exhibits significant variability), so that $z - z_{cb}$ is subject to considerable uncertainty for low in-cloud heights [e.g., *Arabas et al.*, 2009]. This makes it impractical to use measurements of α_l near cloud base as a proxy for $(1 - e/e_c)$. Given these considerations, we use two methods to constrain $(1 - e/e_c)$ with observations. "Method 1" is to use cloud averages of the observed $\alpha_l(z)$ profile $(\alpha_{l,avg})$. This method is expected to provide a lower bound for $(1 - e/e_c)$ because the height dependent factor in equation (4) is always less than unity. In "method 2", a two-parameters least squares fit of equation (4) (to determine e and $(1 - e/e_c)$) to the observed $\alpha_l(z)$ profile is performed. The two fitting parameters chosen for this procedure were e and (e/e_c), subject to the constraints $e \geq 0$ and $0 \leq (e/e_c) \leq 1$. The details of the empirical determination of z_{cb} and of the observed α_l profiles is given in Section 3.

2.3. Impact of Entrainment Parameters on CDNC and Effective Radius

[19] The inferred entrainment parameters, necessary input for the BN07 parameterization, should be such that the predicted CDNC is representative of the observed cloud average CDNC. However, the different methods proposed to estimate this entrainment parameter, have different impacts on the predicted CDNC (as well as in related variables such as the effective radius of the droplet population, r_e). The likely impact of these different approaches in the predicted droplet concentration with BN07 are discussed here and compared against the limits of mixing.

[20] Under adiabatic conditions ($e = 0$), BN07 and FN05 predict the same adiabatic CDNC, denoted N_{ad}. This value is likely to represent an overprediction of the true average CDNC since it does not take into account depletion of CDNC by mixing. N_{ad} exhibits an approximate power law dependence on the updraft velocity, i.e., $N_{ad} \approx aw^b$ (with a, b positive parameters independent of w [*Morales and Nenes*, 2010]). According to BN07, entrainment effects on CDNC can be included by replacing w in the calculation of N_{ad} with $(1 - e/e_c)w$, so the corresponding predicted droplet number concentration under the entrainment rate e, N_e, is $N_e(w) \approx (1 - e/e_c)^b N_{ad}(w)$. Since $(1 - e/e_c) \leq 1$, and $b \leq 1$ for atmospheric aerosol [*Morales and Nenes*, 2010], we obtain the expected $N_e \leq N_{ad}$. The inhomogeneous mixing process, in which all the LWC depletion results from decrease in CDNC (i.e., $N_d \approx \alpha_{l,avg}N_{ad}$), should constitute a lower bound on the actual CDNC. While this inhomogeneous mixing scenario could occur in certain regions in the cloud, it will most likely not be the case for a cloud-scale average CDNC [*Lu et al.*, 2008]. Finally, since $\alpha_{l,avg} \leq (1 - e/e_c)$, the following inequalities for CDNC apply,

$$(\alpha_{l,avg})N_{ad} \leq (\alpha_{l,avg})^b N_{ad} \leq (1 - e/e_c)^b N_{ad} \leq N_{ad} \tag{5}$$

[21] Equation (5) illustrates the expected impact of both methods of introducing entrainment in the BN07 parameterization (i.e., $N_e \approx (\alpha_{l,avg})^b N_{ad}$ for method 1, and $N_e \approx (1 - e/e_c)^b N_{ad}$ for method 2). Each method has the desirable property of being bounded by the inhomogeneous mixing scenario and the adiabatic CDNC. Figure 1 shows schematically how CDNC predicted with these different methods likely compares to observed values.

[22] Observations of cloud-scale averages of microphysical properties in shallow cumulus by *Lu et al.* [2008] are consistent with the above analysis. The cloud-scale ratio of observed to adiabatic CDNC was always greater than the dilution ratio, and for nonprecipitating clouds never exceeds unity, i.e., $(\alpha_{l,avg})N_{ad} < N_{obs} < N_{ad}$.

[23] The discussion above is also consistent with changes in effective radius, r_e, as observed at the cloud scale. Assuming that entrainment effects on the relative dispersion of the droplet size distribution are second order, $r_e/r_{e,ad} \sim (\alpha_l)^{1/3}(N_{ad}/N_e)^{1/3}$ [*Kim et al.*, 2008], where $r_{e,ad}$ is the effective radius computed from N_{ad} and $q_{l,ad}$. In the limit where homogeneous mixing occurs and neglecting the dilution of CNDC due to entrainment it is observed that $N_{ad}/N_e \rightarrow 1$, and $(r_e/r_{e,ad})$ becomes proportional to $\alpha_l^{1/3}$ [e.g., *Kim et al.*, 2008]. In the inhomogeneous mixing limit, $\alpha_l \approx N_e/N_{ad}$, and r_e will, to first order, remain unaffected. If the departure of both N_d and q_l from adiabatic values is accounted for following the formulation previously discussed, then the expected impact on the calculated effective radius would depend on the dilution ratio as, $(r_e/r_{e,ad}) \sim \alpha_l^{(1-b)/3} \leq 1$. These predictions are consistent with the cloud-scale observations of *Lu et al.* [2008], and also fall in between the result under any of the two extreme cases of mixing. All together this suggests that using a entrainment rate diagnosed from the dilution ratio will give q_l profiles, N_d, and r_e consistent with observations. Furthermore, the treatment proposed here allows for a nonlinear relation between α_l and N_d.

3. Cloud Observations Used for the Evaluation

[24] The data sets used in this study were collected using the CIRPAS Twin Otter aircraft during the CRYSTAL-FACE (Key West, Florida, July 2002) and CSTRIPE (Monterey, California, 2003) field campaigns. CRYSTAL-FACE focused on cumulus clouds, while CSTRIPE addressed stratocumulus clouds off the California coast. These sets have been used in several studies of cloud microphysics and aerosol-cloud interactions, including an aerosol-CCN closure [*VanReken et al.*, 2003], aerosol-CDNC closure [*Conant et al.*, 2004; *Meskhidze et al.*, 2005], autoconversion parameterization evaluation [*Hsieh et al.*, 2009b] and comparisons between observed and predicted droplet size distributions [*Hsieh et al.*, 2009a]. Descriptions of the instrumentation, sampling techniques and analysis are provided in the aforementioned studies; only a brief description of the data relevant for evaluation of the activation parameterization is given here.

[25] A total of 8 stratocumulus decks sampled during the CSTRIPE campaign (including the 52 in-cloud transects considered by *Meskhidze et al.* [2005]), and 18 cumulus clouds (143 in-cloud transects) observed during CRYSTAL-FACE are considered in this study. Cloud microphysical properties were sampled at 1 Hz frequency using a Forward Scattering Spectrometer Probe (FSSP) in a series of horizontal in-cloud transects. The horizontal sampling transects were performed at heights ranging from near cloud base to cloud top, spanning most of the cloud depth. Vertical profiles of CDNC and liquid water content were then reconstructed from the FSSP measurements. Examples of the typical LWC profiles observed in these clouds are included in Figure 2. Updraft velocity measurements were performed with a five-hole turbulence probe. The cloud-scale average CDNC reported in this study was calculated as an average over the total number of CDNC data points for each cloud as derived from the FSSP measurements.

[26] The entrainment parameter, $(1 - e/e_c)$, is constrained using the methods described in Section 2.2, both requiring observed values of α_l at different in-cloud heights. The adiabatic liquid water content lapse rate, $\Gamma_{l,ad}$, was calculated from the measured temperature and pressure. Cloud base height, z_{cb}, was estimated by extrapolating the LWC measured at the lower cloud penetrations, assuming those points followed the linear profile given by adiabatic condensation, $q_{l,ad} = \Gamma_{l,ad}(z - z_{cb})$. Estimation of cloud base with this method has been used in other studies [e.g., *Peng et al.*, 2002]. Once z_{cb} is determined, estimation of the dilution ratio α_l at the observation height z, was done by dividing the observed liquid water content $q_{l,obs}(z)$ at height z, with the expected adiabatic value, i.e., $\alpha_l(z) \approx q_{l,obs}(z)/q_{l,ad}(z)$ for each observed LWC data point. After completing these steps, near cloud base data points were discarded and only the remaining data points were used in the calculations of $\alpha_{l,avg}$ (method 1, applied to both data sets), or for the fittings to equation (4) of method 2 (which was only applied to the CRYSTAL-FACE cumulus). This was done to minimize the impact of cloud base uncertainty in estimation of α_l and $(1 - e/e_c)$.

[27] Figure 2 presents examples of typical LWC profiles observed for clouds in CRYSTAL-FACE and CSTRIPE. Also shown are the estimated $q_{l,ad}(z)$ and the fitted $q_l(z)$ for the cumulus case. The frequency distribution of α_l in the stratocumulus layers was observed to consist of a single mode with the peak very close to the mean value (inset of Figure 2, left). In cumulus clouds, the distribution was much broader, characterized by frequent mixing and relatively infrequent adiabatic parcels. Tables 1 and 2 summarize the observed and inferred parameters for all the clouds included in this study.

4. Parameterization Evaluation

[28] Prediction of CDNC with physically based parameterizations such as FN05 or BN07 requires input from observations of the conditions under which activation takes place. This input consist on below-cloud thermodynamic data (pressure and temperature), aerosol size distribution and chemical composition, updraft velocity, and in the case of BN07, the entrainment parameter $(1 - e/e_c)$. The aerosol size distributions were fitted to four-mode lognormal distributions, assuming a composition of pure ammonium sulfate [*Meskhidze et al.*, 2005]. Following one of the methods suggested by *Meskhidze et al.* [2005], a probability density function (PDF) of updraft velocities, $p(w)$, constructed from the turbulence probe measurements in the stratocumulus

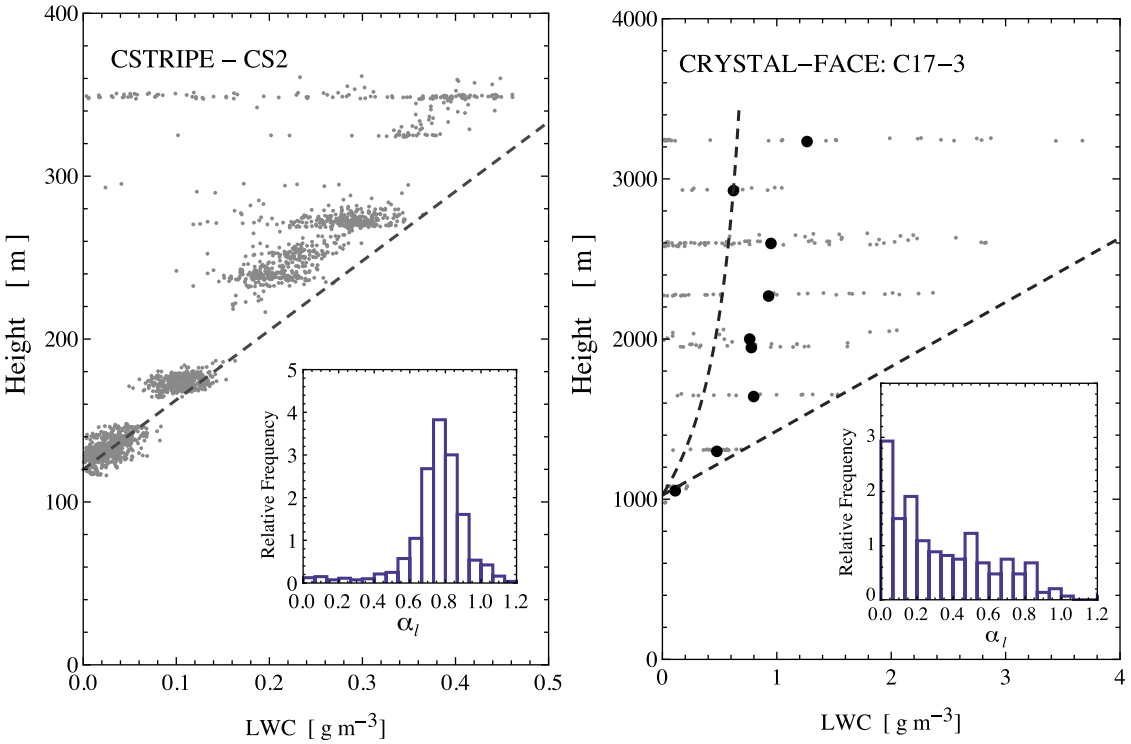

Figure 2. Typical liquid water content profiles observed during the CSTRIPE and CRYSTAL-FACE campaigns for (left) stratocumulus deck (CS2) and (right) cumulus cloud (C17-3). Dashed straight lines correspond to adiabatic liquid water profile $q_{l,ad}(z)$. For the cumulus case (Figure 2, right), the curved dashed line is the equation (4) fit to the observed 1Hz $q_l(z)$ (gray dots). Black dots are the transect average $q_l(z)$. The inset in each plot is the relative frequency distribution of α_1.

decks was used to predict an average $N_d = \frac{\int_0^\infty wp(w)N_e(w)\mathrm{d}w}{\int_0^\infty wp(w)\mathrm{d}w}$, where $N_e(w)$ is the CDNC predicted with BN07 for the updraft w. A single updraft velocity (equal to the average updraft at cloud base) was used in the calculation of CDNC for CRYSTAL-FACE cumulus clouds. Finally, we also compared BN07 against the *Leaitch et al.* [1996] statistical correlation (given by $N_e = 0.1N_{ad}^{1.27}$), using FN05 to predict N_{ad}.

5. Analysis and Discussion of Results

[29] For some of the CSTRIPE stratocumulus cloud layers, LWC exhibited significant deviations from adiabatic values; this however did not occur frequently enough to strongly impact CDNC. Figure 3a presents the predicted adiabatic CDNC against the cloud-scale average observed CDNC. No significant bias was observed (relative error of 4.2 ± 19%), and most of the 8 stratocumulus decks sampled

Table 1. Cloud Average Cloud Droplet Number Concentration (N_d) and Dilution Ratio ($\alpha_{l,avg}$) for the CSTRIPE Stratocumulus Clouds Considered in This Study[a]

Cloud	Date	N_d (cm^{-3})	$\alpha_{l,avg}$
CS1	18 July	432 ± 112	0.62 ± 0.12
CS2	21 July	299 ± 116	0.75 ± 0.17
CS3	22 July	401 ± 129	0.76 ± 0.08
CS4	23 July	316 ± 113	0.54 ± 0.19
CS5	24 July	399 ± 152	0.76 ± 0.37
CS6	25 July	293 ± 112	0.29 ± 0.09
CS7	26 July	394 ± 162	0.53 ± 0.12
CS8	27 July	429 ± 134	0.50 ± 0.16

[a]Uncertainties for each parameter correspond to one standard deviation from the mean. Cloud identifiers follow *Meskhidze et al.* [2005].

Table 2. Cloud Average Cloud Droplet Number Concentration (N_d), Dilution Ratio ($\alpha_{l,avg}$), and ($1 - e/e_c$) (Estimated With Method 2) for the CRYSTAL-FACE Clouds Considered in This Study[a]

Cloud	N_d (cm^{-3})	$\alpha_{l,avg}$	$1 - e/e_c$
H04-1	568 ± 222	0.71 ± 0.38	1.00
H04-2	617 ± 293	0.59 ± 0.36	1.00
H04-3	377 ± 79	0.57 ± 0.27	0.51
C06-1	207 ± 101	0.39 ± 0.33	0.60
C06-2	250 ± 117	0.33 ± 0.28	0.64
C06-3	274 ± 154	0.29 ± 0.23	0.73
C08-1	766 ± 420	0.31 ± 0.23	0.33
C08-2	586 ± 325	0.27 ± 0.21	0.42
C10-1	1158 ± 681	0.43 ± 0.44	0.43
C11-1	1147 ± 517	0.38 ± 0.24	0.68
C11-2	1745 ± 1129	0.62 ± 0.69	1.00
C12-1	305 ± 154	0.31 ± 0.24	0.54
C12-2	349 ± 177	0.33 ± 0.25	0.36
C16-1	219 ± 96	0.53 ± 0.39	1.00
C16-2	197 ± 93	0.44 ± 0.38	0.64
C17-1	325 ± 140	0.63 ± 1.11	1.00
C17-2	262 ± 130	0.36 ± 0.33	0.38
C17-3	284 ± 189	0.37 ± 0.35	1.00

[a]Uncertainties for each parameter correspond to one standard deviation from the mean. Cloud identifiers follow *Meskhidze et al.* [2005].

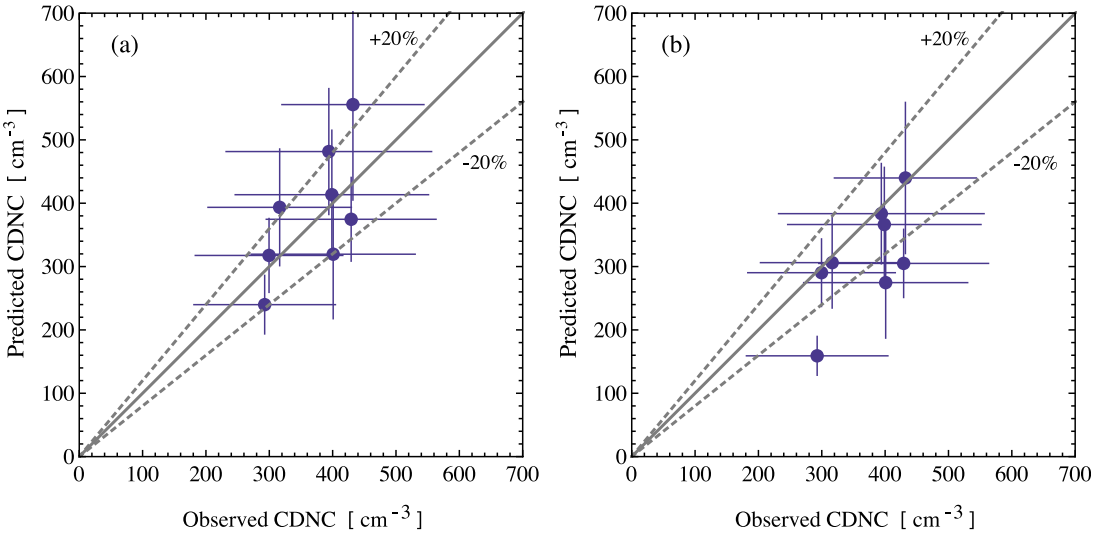

Figure 3. Comparison between observed cloud-scale average CDNC and predicted CDNC for CSTRIPE clouds with (a) FN05 parameterization and (b) BN07 parameterization with $(1 - e/e_c)$ estimated as the cloud average α_1 (method 1). Horizontal error bars represent one standard deviation of 1 Hz FSSP data. Vertical error bars are one standard deviation in predicted CDNC, as calculated from the observed PDF of updraft velocities.

were predicted within the ±20% uncertainty of the FSSP measurements. Conversely, applying BN07 with method 1 (Figure 3b) exhibits modest underprediction of CDNC, with a relative error of −15 ± 17%. The vertical error bars were estimated as the variance in CDNC expected from the variability in vertical velocity, i.e., $\sigma^2 = \int wp(w)(N_d(w) - N_d)^2 dw / \int wp(w)dw$.

[30] When the adiabatic CDNC was compared to the cloud-scale average CDNC for the CRYSTAL-FACE cumulus clouds, a significant overprediction (31 ± 39%) of CDNC was observed (Figure 4a). Application of BN07 substantially improves the predictions, with an average error of −3.5 ± 23%, using $(1 - e/e_c)$ calculated from method 1 (Figure 4a). If method 2 is used, the relative error between predictions and observations is equal to 14 ± 31%. For a comparison with observations assuming inhomogeneous entrainment (IH), in which all the liquid water depletion (from the adiabatic expected values) is attributed to reduction of the total

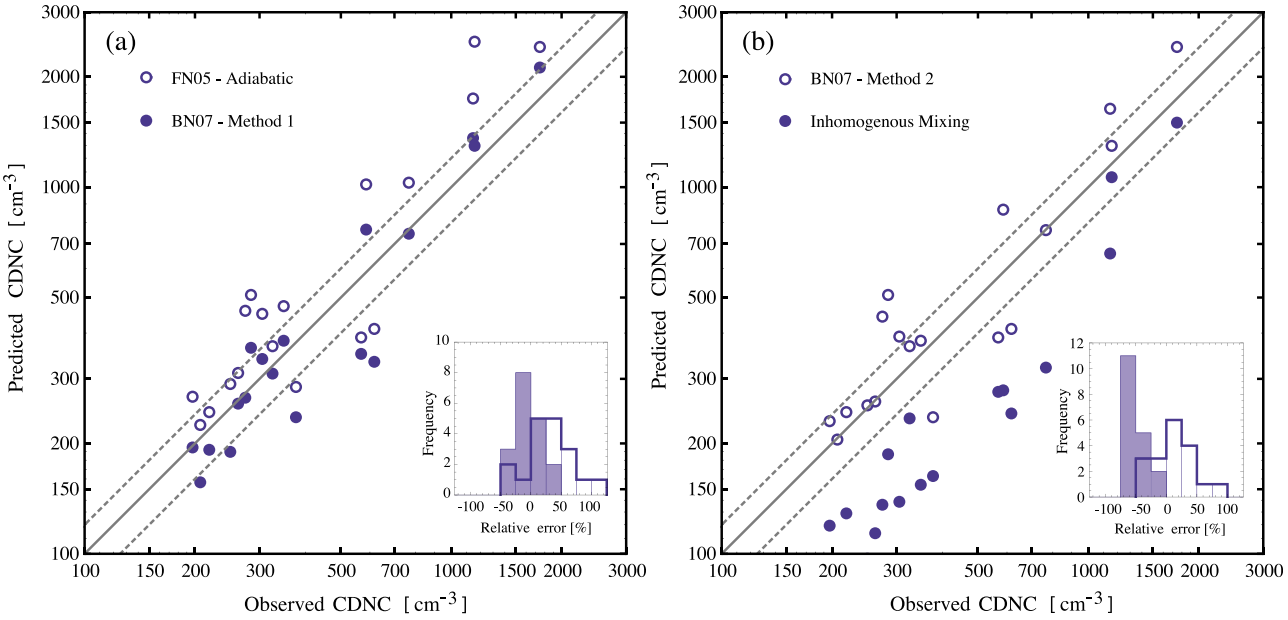

Figure 4. Comparison between cloud average observed CDNC and predicted CDNC for 18 clouds sampled during CRYSTAL-FACE. Shown are predictions of CDNC using (a) FN05 and BN07 with $(1 - e/e_c)$ estimated as the column average α_1 (method 1) and (b) BN07 parameterization with $(1 - e/e_c)$ estimated from method 2 and IH scenario where $N_d \approx (\alpha_{1,avg})N_{ad}$. The insets are the frequency histograms for the relative error between predictions and observations.

CDNC, i.e., $N_d \approx \alpha_{l,avg} N_{ad}$, CDNC was significantly underpredicted, on average by $-45 \pm 15\%$. Compared to the statistical approach of *Leaitch et al.* [1996], BN07 provided a much better representation of cloud-scale average CDNC, as the former underpredicted N_d by -24% for CRYSTAL-FACE and $-45\% \pm 13\%$ for CSTRIPE clouds.

[31] Following *Burnet and Brenguier* [2006], the volume mean diameters, D_v, and CDNC derived from the 1Hz FSSP measurements were analyzed with their proposed $D_v - N_d$ diagram to establish the extent to which the data follow a clear preferential type of mixing (either homogeneous or inhomogeneous). The data from the CSTRIPE stratocumulus tended to align along the constant α_l lines (consistent with the observed frequency distributions showed in Figure 2 and $\alpha_{l,avg}$ presented in Table 1), while the CRYSTAL-FACE cumulus data points spanned the entire thermodynamically allowed space in the diagram, not exhibiting any specific trend (not shown). Since this study is concerned only with cloud-scale averages of CDNC, $\alpha_{l,avg}$ inferred from the observations expresses a convolution of homogeneous and inhomogeneous mixing across multiple scales.

5.1. CSTRIPE Data

[32] The entrainment and mixing process in the cloud-topped marine boundary layer is highly concentrated in the vicinity of the overlaying inversion, away from the activation zones near cloud base. Generally, the most dilute parcels are distributed in the upper part of the cloud adjacent to the temperature inversion, where they are exposed to cloud top entrainment, and represent a relatively small fraction of the cloudy air mass volume (Figure 2, left). Therefore, the good agreement between observed cloud averaged CDNC with the adiabatic parameterization (Figure 3a) is not surprising. Furthermore, since the marine boundary layer is generally well mixed, and the cloud base for all the cases occurred between 150 and 300 m above sea level, the below-cloud layer was near saturation; thus minimizing entrainment effects near cloud base.

5.2. CRYSTAL-FACE Data

[33] The small and moderately sized cumulus clouds sampled during the CRYSTAL-FACE campaign were observed to have highly diluted parcels throughout the cloud column (Figure 2, right). This is consistent with the model of clouds growing in a dryer environment, with stronger vortical motions that engulf cloud-free air. Contrary to the marine stratocumulus clouds of the CSTRIPE campaign, a strong correlation between CDNC and α_l is observed. Since entrainment is more likely to deplete the CDNC throughout the entire cloud column in a cumulus cloud, significant overprediction of CDNC with the adiabatic parameterization is expected (as the adiabatically predicted CDNC represents an upper bound on the expected CDNC).

[34] As discussed in section 2.3, agreement between predicted and observed CDNC for the CRYSTAL-FACE cumuli using BN07 is expected if the observed CDNC results from a balance between the two extremes of mixing. The assumption that cloud-scale averaged CDNC is equal to the adiabatically predicted value, N_{ad}, constitutes an upper limit and most likely is an overestimate of N_d (because of neglect of the diluting effect of entrainment and mixing), and the inhomogeneous mixing limit is unlikely to be representative of cloud-scale averages of CDNC. This is confirmed by the closure calculations, as N_{ad} overpredicts the observed CDNC by 31% (Figure 3a), and $\alpha_{l,avg} N_{ad}$ underestimates CDNC by 45% (Figure 3b).

[35] Figure 4 supports the inequalities presented in equation (5), since the respective biases of both methods are much smaller than for both the IH mixing and the adiabatic scenario. It is also possible that the overestimation of e/e_c with method 1 partially compensates for increased entrainment and mixing at cloud top (unaccounted for under the assumption of constant e used in equation (3)), explaining the better closure when this method is employed. The simplified approach presented here does not include a detailed analysis of the nature of the entrainment process itself, but it appears capable of effectively correcting the overprediction of the average CDNC in ambient clouds when N_d is assumed to be equal to the number of adiabatically activated droplets. The results presented here are also consistent with other observations of microphysical properties at the cloud scale [*Peng et al.*, 2002].

6. Conclusions

[36] Cloud droplet number concentration predicted with the BN07 activation parameterization was evaluated against measurements of CDNC in cumulus and stratocumulus clouds sampled during the CSTRIPE and CRYSTAL-FACE campaigns. It was shown that BN07 performed better than adiabatically predicted CDNC (with FN05) for the cloud-averaged CDNC in cumulus clouds, correcting a systematic overprediction bias of 31%. In stratocumulus clouds, inclusion of entrainment effects did not further improve the CDNC closure; this is consistent with the conceptual model of a well-mixed boundary layer capped by a strong temperature inversion. In all cases considered, BN07 compared favorably against a statistical correlation developed from observations to treat entrainment effects on droplet number.

[37] Different methods to estimate the impact of entrainment and mixing on the CDNC were explored, finding that BN07 predicts CDNC within the limits imposed by the inhomogeneous mixing lower limit and the adiabatic upper limit. The agreement between observed and predicted CDNC when entrainment effects are included (by setting $(1 - e/e_c)$ equal to the average dilution ratio, α_l) suggest that the simple scheme presented here is a possible way to effectively account for the impact of entrainment on average cloud microphysical properties.

[38] An evaluation such as that in the present study should be repeated with other field campaign data, especially under clean conditions (where the dependence of N_d on w could be substantially different from the conditions considered here). Nevertheless, the results presented here strongly support that BN07 can correct an important source of CDNC overprediction bias in large-scale atmospheric models, and are in good agreement with observational studies of continental cumulus.

[39] **Acknowledgments.** We acknowledge support from NASA-ACMAP, NSF-CAREER, and ONR (grant N00014-10-1-0200). We also thank Donifan Barahona, Jeff Snider, and two anonymous reviewers for comments that improved the manuscript.

References

Abdul-Razzak, H., S. Ghan, and C. Rivera-Carpio (1998), A parameterization of aerosol activation: 1. Single aerosol type, *J. Geophys. Res.*, *103*, 6123–6131.

Arabas, S., H. Pawlowska, and W. W. Grabowski (2009), Effective radius and droplet spectral width from in-situ aircraft observations in trade-wind cumuli during RICO, *Geophys. Res. Lett.*, *36*, L11803, doi:10.1029/2009GL038257.

Baker, M. B., R. G. Corbin, and J. Latham (1980), The influence of entrainment on the evolution of cloud droplet spectra: I. A model of inhomogenous mixing, *Q. J. R. Meteorol. Soc.*, *106*, 581–598.

Barahona, D., and A. Nenes (2007), Parameterization of cloud droplet formation in large-scale models: Including effects of entrainment, *J. Geophys. Res.*, *112*, D16206, doi:10.1029/2007JD008473.

Barahona, D., R. E. L. West, P. Stier, S. Romakkaniemi, H. Hokkola, and A. Nenes (2010), Comprehensively accounting for the effect of giant CCN in cloud activation parameterizations, *Atmos. Chem. Phys.*, *10*, 2467–2473.

Barahona, D., R. E. P. Sotiropoulou, and A. Nenes (2011), Global distribution of cloud droplet number concentration, autoconversion rate, and aerosol indirect effect under diabatic droplet activation, *J. Geophys. Res.*, *116*, D09203, doi:10.1029/2010JD015274.

Burnet, F., and J.-L. Brenguier (2006), Observational study of the entrainment-mixing process in warm convective clouds, *J. Atmos. Sci.*, *64*, 1995–2011, doi:10.1175/JAS3928.1.

Chosson, F., J.-L. Brenguier, and L. Schüller (2006), Entrainment-mixing and radiative transfer simulation in boundary layer clouds, *J. Atmos. Sci.*, *64*, 2670–2682, doi:10.1175/JAS3975.1.

Conant, W. C., et al. (2004), Aerosol-cloud drop conentration closure in warm cumulus, *J. Geophys. Res.*, *109*, D13204, doi:10.1029/2003JD004324.

de Rooy, W. C., and P. Siebesma (2010), Analytical expressions for entrainment and detrainment in cumulus convection, *Q. J. R. Meteorol. Soc.*, *136*, 1216–1227, doi:10.1002/qj.640.

Fountoukis, C., and A. Nenes (2005), Continued development of a cloud droplet formation parameterization for global climate models, *J. Geophys. Res.*, *110*, D11212, doi:10.1029/2004JD005591.

Fountoukis, C., et al. (2007), Aerosol-cloud drop concentration closure for clouds sampled during the International Consortium for Atmospheric Research on Transport and Transformation 2004 campaign, *J. Geophys. Res.*, *112*, D10S30, doi:10.1029/2006JD007272.

Hsieh, W. C., A. Nenes, R. C. Flagan, J. H. Seinfeld, G. Buzorius, and H. Jonsson (2009a), Parameterization of cloud droplet size distributions: Comparison with parcel models and observations, *J. Geophys. Res.*, *114*, D11205, doi:10.1029/2008JD011387.

Hsieh, W. C., H. Jonsson, L.-P. Wang, G. Buzorius, R. C. Flagan, J. H. Seinfeld, and A. Nenes (2009b), On the representation of droplet coalescence and autoconversion: Evaluation using ambient cloud droplet size distributions, *J. Geophys. Res.*, *114*, D07201, doi:10.1029/2008JD010502.

Intergovernmental Panel on Climate Change (2007), Summary for policymakers, in *Climate Change* 2007*: The Physical Science Basis: Working Group I Contribution to the Fourth Assessment Report of the Intergovernmental Panel on Climate Change*, edited by S. Solomon et al., pp. 1–18, Cambridge Univ. Press, New York.

Khairoutdinov, M., and Y. Kogan (2000), A new cloud physics parameterization in a large-eddy simulation model of marine stratocumulus, *Mon. Weather Rev.*, *128*, 229–243.

Kim, B.-G., M. A. Miller, S. E. Schwartz, Y. Liu, and Q. Min (2008), The role of adiabaticity in the aerosol first indirect effect, *J. Geophys. Res.*, *113*, D05210, doi:10.1029/2007JD008961.

Krueger, S. K., C.-W. Su, and P. A. McMurtry (1997), Modeling entrainment and finescale mixing in cumulus clouds, *J. Atmos. Sci.*, *54*, 2697–2712.

Kumar, P., I. N. Sokolik, and A. Nenes (2009), Parameterization of cloud droplet formation for global and regional models: Including adsorption activation from insoluble CCN, *Atmos. Chem. Phys.*, *9*, 2517–2532.

Lasher-Trapp, S. G., W. A. Cooper, and A. M. Blyth (2005), Broadening of droplet size distributions from entrainment and mixing in a cumulus cloud, *Q. J. R. Meteorol. Soc.*, *131*, 195–220, doi:10.1256/qj.03.199.

Latham, J., and R. L. Reed (1977), Laboratory studies of the effects of mixing on the evolution of cloud droplet spectra, *Q. J. R. Meteorol. Soc.*, *103*, 297–306.

Leaitch, W. R., C. M. Banic, G. A. Isaac, M. D. Couture, P. S. K. Lius, I. Gultepe, S. M. Li, L. Kleinman, P. H. Daum, and J. I. MacPherson (1996), Physical and chemical observations in marine stratus during the 1993 North Atlantic Regional Experiment: Factors controlling cloud droplet number concentrations, *J. Geophys. Res.*, *101*, 29,123–29,135.

Lehmann, K., H. Siebert, and R. A. Shaw (2009), Homogeneous and inhomogeneous mixing in cumulus clouds: Dependence on local turbulence structure, *J. Atmos. Sci.*, *66*, 3641–3659, doi:10.1175/2009JAS3012.1.

Liu, Y., P. H. Daum, H. Guo, and Y. Peng (2008), Dispersion bias, dispersion effect, and the aerosol-cloud conundrum, *Environ. Res. Lett.*, *3*, 045021, doi:10.1088/1748-9326/3/4/045021.

Lohmann, U. (2008), Global anthropogenic aerosol effects on convective clouds in ECHAM5-HAM, *Atmos. Chem. Phys.*, *8*, 2115–2131.

Lu, M.-L., G. Feingold, H. H. Jonsson, P. Y. Chuang, H. Gates, R. C. Flagan, and J. H. Seinfeld (2008), Aerosol-cloud relationships in continental shallow cumulus, *J. Geophys. Res.*, *113*, D15201, doi:10.1029/2007JD009354.

Meskhidze, N., A. Nenes, W. C. Conant, and J. H. Seinfeld (2005), Evaluation of a new cloud droplet activation parameterization with in situ data from CRYSTAL-FACE and CSTRIPE, *J. Geophys. Res.*, *110*, D16202, doi:10.1029/2004JD005703.

Ming, Y., V. Ramaswamy, L. J. Donner, and V. T. J. Phillips (2006), A new parameterization of cloud droplet activation applicable to general circulation models, *J. Atmos. Sci.*, *63*, 1348–1356.

Morales, R., and A. Nenes (2010), Characteristic updrafts for computing distribution-averaged cloud droplet number and stratocumulus cloud properties, *J. Geophys. Res.*, *115*, D18220, doi:10.1029/2009JD013233.

Morrison, H., and A. Gettelman (2008), A new two-moment bulk stratiform cloud microphysics scheme in the Community Atmosphere Model, Version 3 (CAM3). Part I: Description and numerical tests, *J. Clim.*, *21*, 3642–3659, doi:10.1175/2008JCLI2105.1.

Nenes, A., and J. H. Seinfeld (2003), Parameterization of cloud droplet formation in global climate models, *J. Geophys. Res.*, *108*(D14), 4415, doi:10.1029/2002JD002911.

Peng, Y., U. Lohmann, R. Leaitch, C. Banic, and M. Couture (2002), The cloud albedo-cloud droplet effective radius relationship for clean and polluted clouds from RACE and FIRE.ACE, *J. Geophys. Res.*, *107*(D11), 4106, doi:10.1029/2000JD000281.

Pruppacher, H. R., and J. D. Klett (1997), *Microphysics of Clouds and Precipitation*, 2nd ed., Kluwer Acad., Boston, Mass.

Stevens, B., and G. Feingold (2009), Untangling aerosol effects on clouds and precipitation in a buffered system, *Nature*, *461*, 607–613, doi:1038/nature08281.

Tiedtke, M. (1989), A comprehensive mass flux scheme for cumulus parameterization in large-scale models, *Mon. Weather Rev.*, *117*, 1779–1800.

Twomey, S. (1959), The nuclei of natural cloud formation. Part II: The supersaturation in natural clouds and the variation of cloud droplet concentration, *Geofis. Pura Appl.*, *43*, 243–249.

VanReken, T. M., T. A. Rissman, G. C. Roberts, V. Varutbangkul, H. H. Jonsson, R. C. Flagan, and J. H. Seinfeld (2003), Toward aerosol/cloud condensation nuclei (CCN) closure during CRYSTAL-FACE, *J. Geophys. Res.*, *108*(D20), 4633, doi:10.1029/2003JD003582.

Warner, J. (1970), On steady-state one-dimensional models of cumulus convection, *J. Atmos. Sci.*, *27*, 1035–1040.

Warner, J. (1973), Microstructure of cumulus clouds: Part IV: The effect on the droplet spectrum of mixing between cloud and environment, *J. Atmos. Sci.*, *30*, 256–261.

R. C. Flagan and J. H. Seinfeld, Department of Chemical Engineering, California Institute of Technology, Pasadena, CA 91125, USA. (flagan@cheme.caltech.edu; seinfeld@caltech.edu)

H. Jonsson, Center for Interdisciplinary Remotely Piloted Aircraft Studies, Naval Postgraduate School, Monterey, CA 93943, USA. (hjonsson@nps.edu)

R. Morales, School of Earth and Atmospheric Sciences, Georgia Institute of Technology, 311 Ferst Dr., Atlanta, GA 30332-0340, USA. (ricardo.morales@gatech.edu)

A. Nenes, School of Chemical and Biomolecular Engineering, Georgia Institute of Technology, 311 Ferst Dr., Atlanta, GA 30332-0340, USA. (athanasios.nenes@gatech.edu)